Applications of Magnetic Separation

J.H.P. Watson

University of Southampton, Southampton, UK
jhpw@soton.ac.uk

Separation of bone marrow stem cells

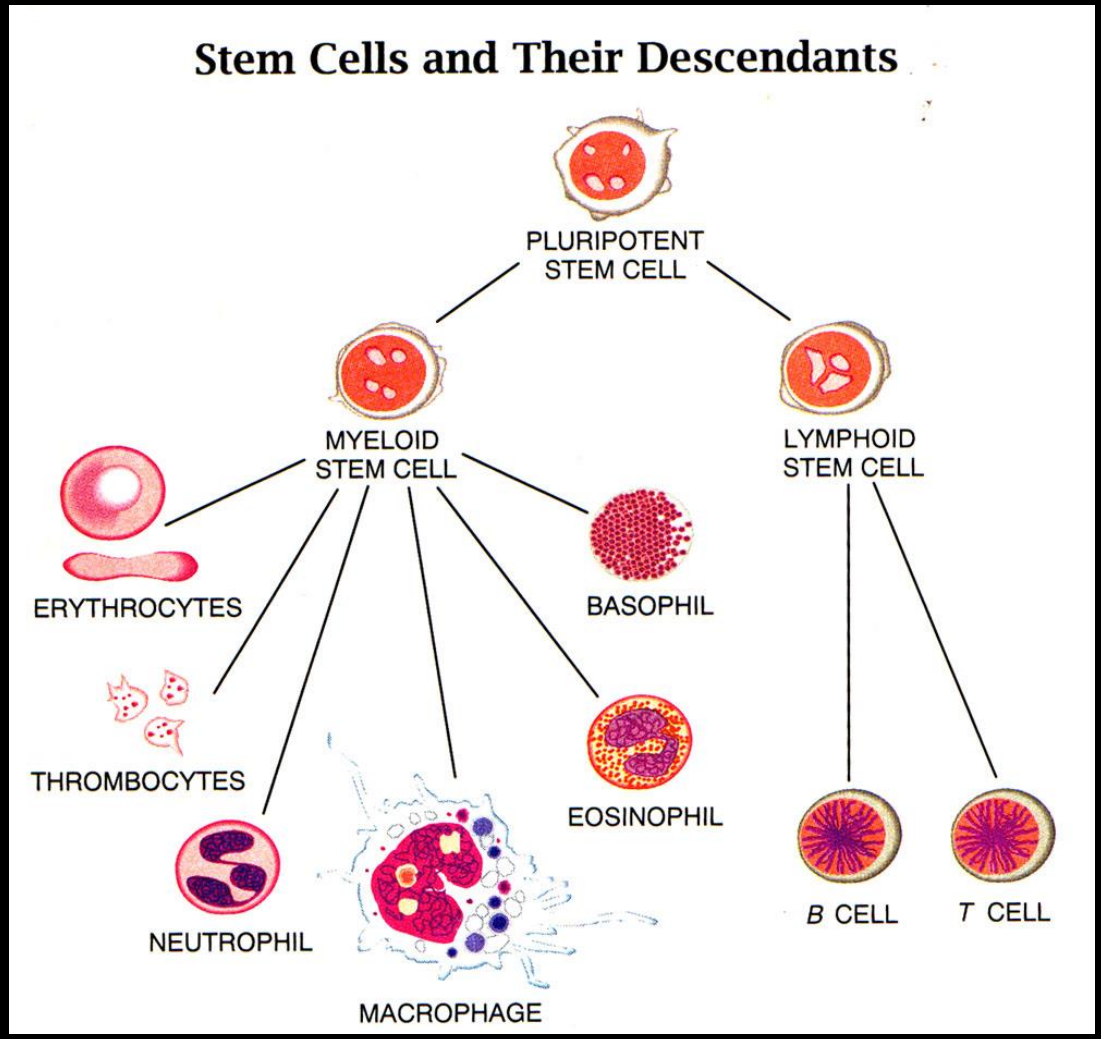

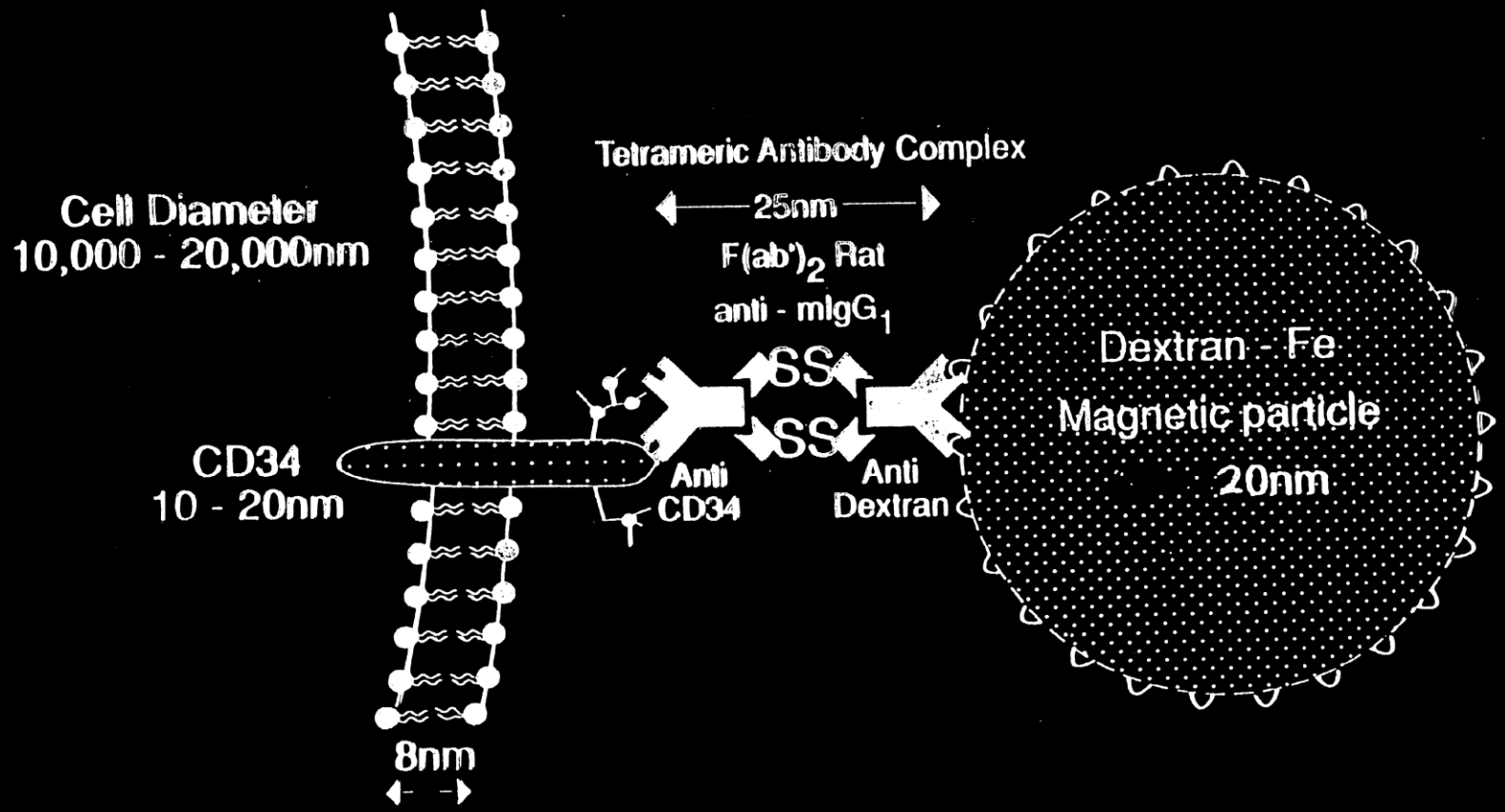

Labelling of a CD34 positive cell by a tetrameric antibody complex and a dextran-iron particle. The diagram was kindly provided by Dr T.E. Thomas of the Terry Fox Laboratory.

Electron Microscope scan

A Scanning Electron Microscope (SEM) picture of magnetically separated CD8 positive, previously cryopreserved cells. The sample was 90% CD8 positive and 6% of the cells were dead. The photograph was not representative, it was chosen so that each of the cell types would be represented i.e. lymphocytes, monocytes, dead cells and cell fragments. The size bar should not be taken as true since some shrinkage of the cells occurred during preparation.

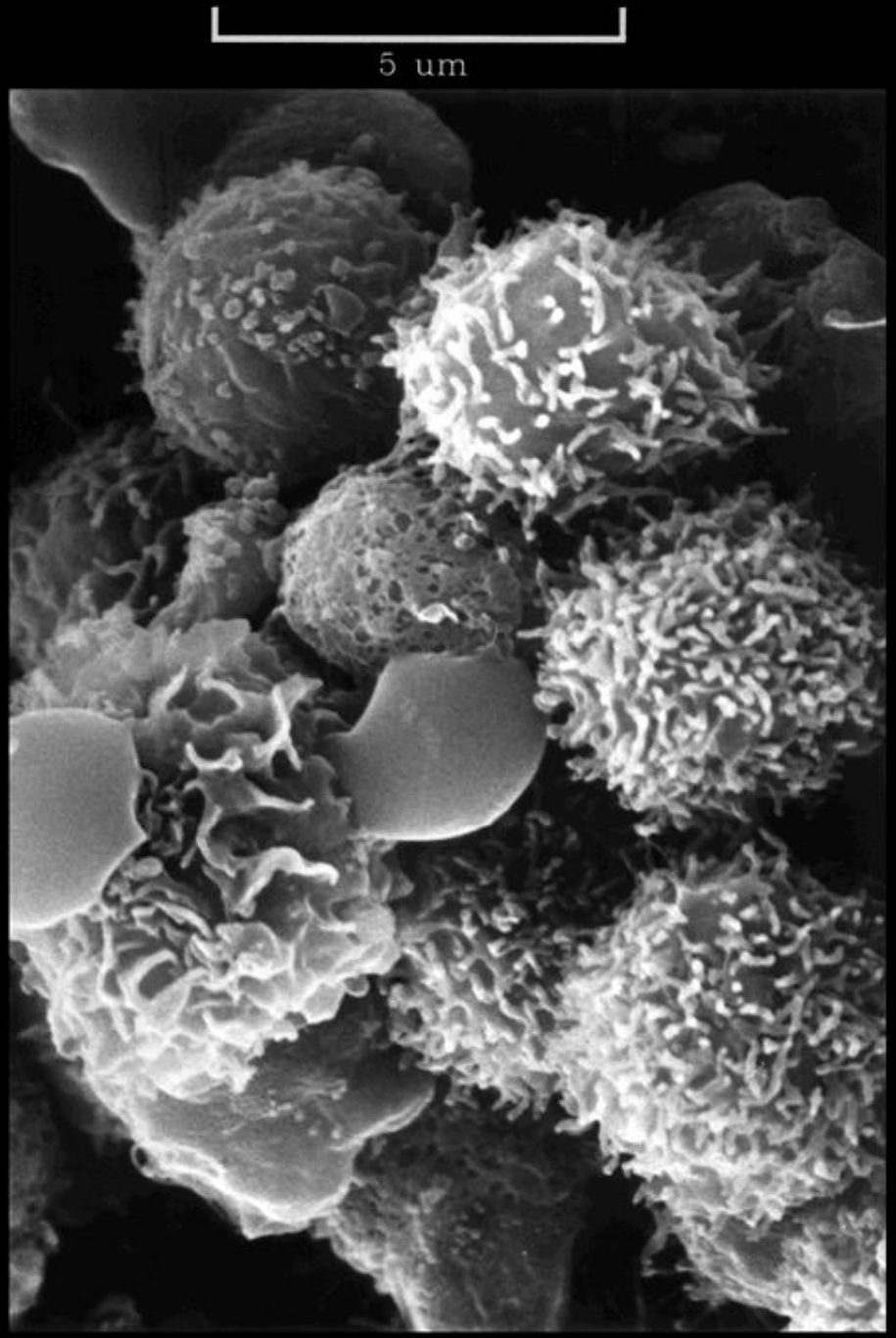

Magnetisation of tagged cells and of iron dextran

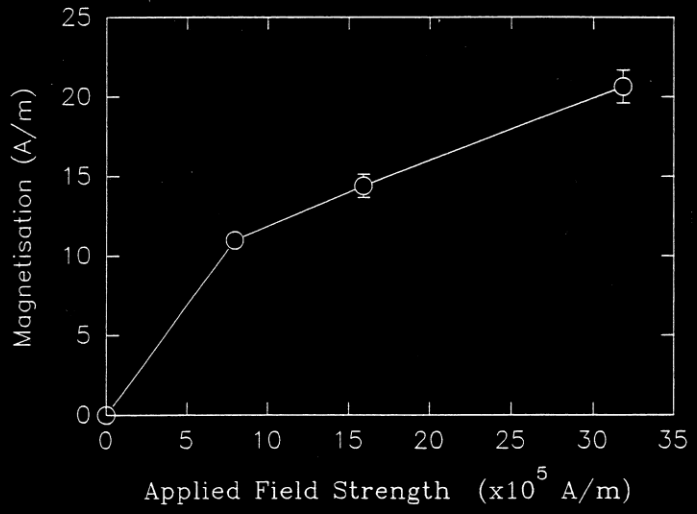

The magnetisation curve of cells labelled with CD34 tetrameric antibody complexes and dextran-iron particles. The cells were previously cryopreserved peripheral blood mononuclear cells derived from three donors. The curve was corrected for unlabelled cells and the aqueous suspending media.

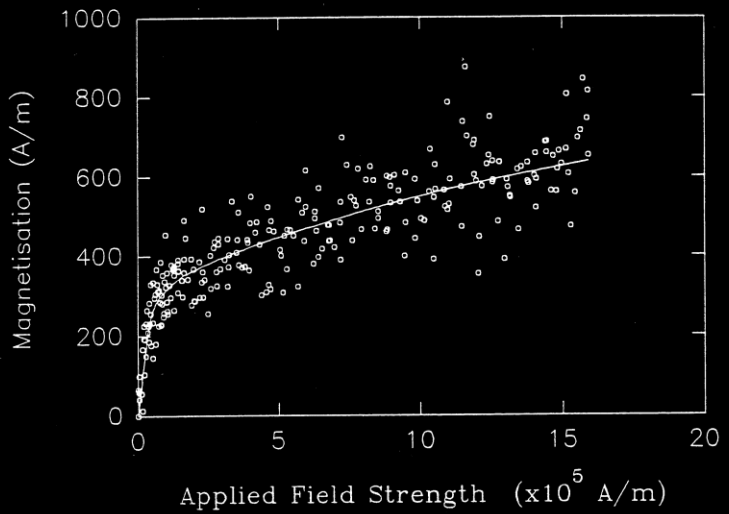

The magnetisation curve of a suspension of Dextran-Iron particles with OD_{450nm}=6.2. There were 250 data points and the sample was approximately 0.08 g.

Capture radius versus V_m/V_o

R_{ca} versus V_m/V_o graph for CD34 positive cells from bone marrow. Three, zero to two day old fresh donors over nine separations and four previously cryopreserved donors over 6 separations were used. The CD34 antibodies used were 8G12 over 5 separations and 14G3 over 10 separations.

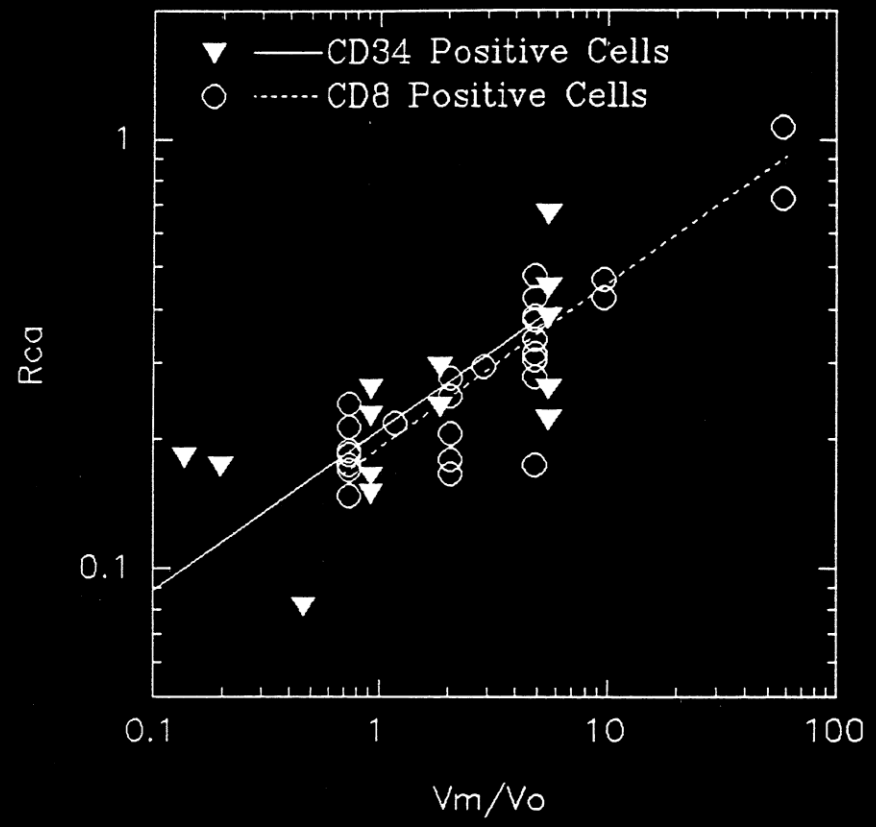

Purity and Recovery

The purities were strongly influenced by the amount of negative cell retention in the filter. The retention due to the filter at zero magnetic field had been reduced to the minimum practical level. The dominant area for negative cell retention was adherence and lodgement amongst the positive cells retained on the wire array.

At the second 1 T separation these troublesome negative cells were only a small fraction of the total cells in the feed:

0.5% mean, 0.1-2.3% range, the monocytes solely contributing to the higher values.

It was theoretically demonstrated that to achieve purities >98% for many practical cell separation applications, multiple successive separations were required. Despite the small subpopulation of highly adhesive negative cells, purities after the second separation were:

97.6% mean, 96.0-98.3% range for 5 previously cryopreserved donors over 5 separations.

In the only two experiments where a third separation was performed the purity was >99%.

Canister cross-section

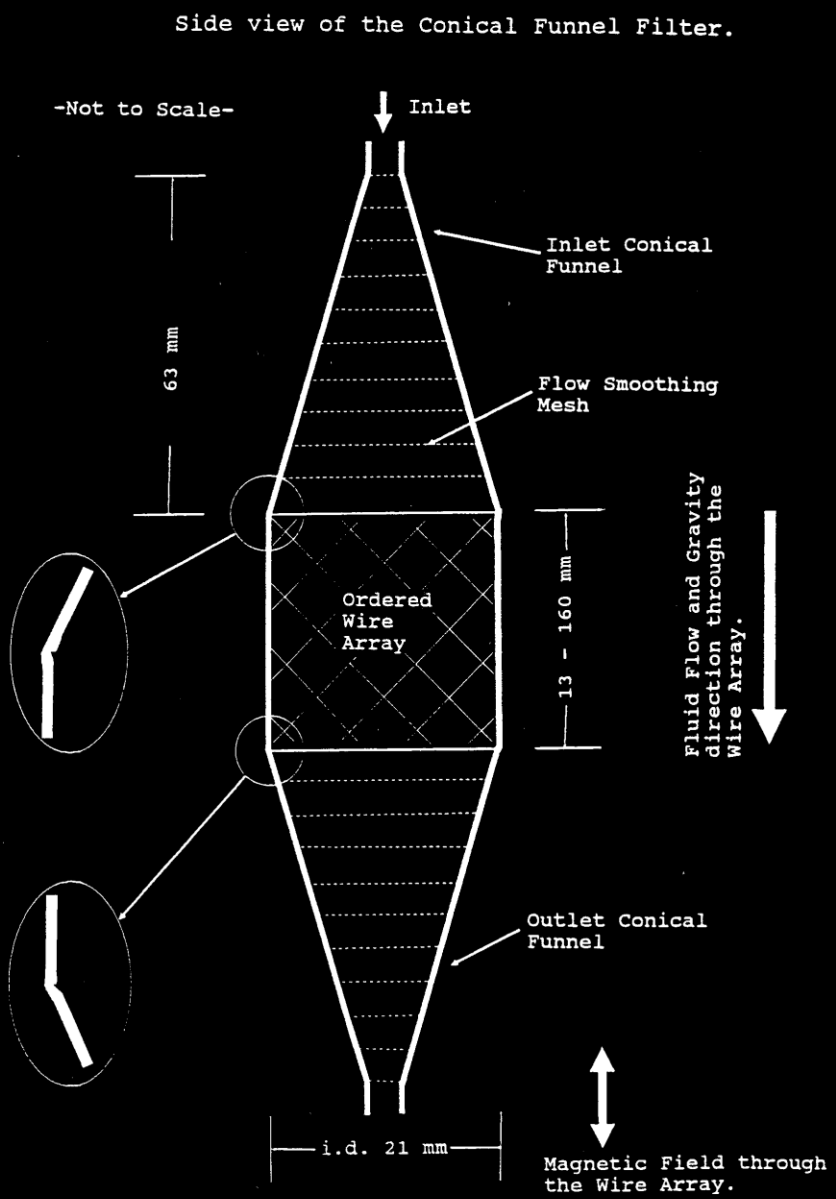

The canister and matrix

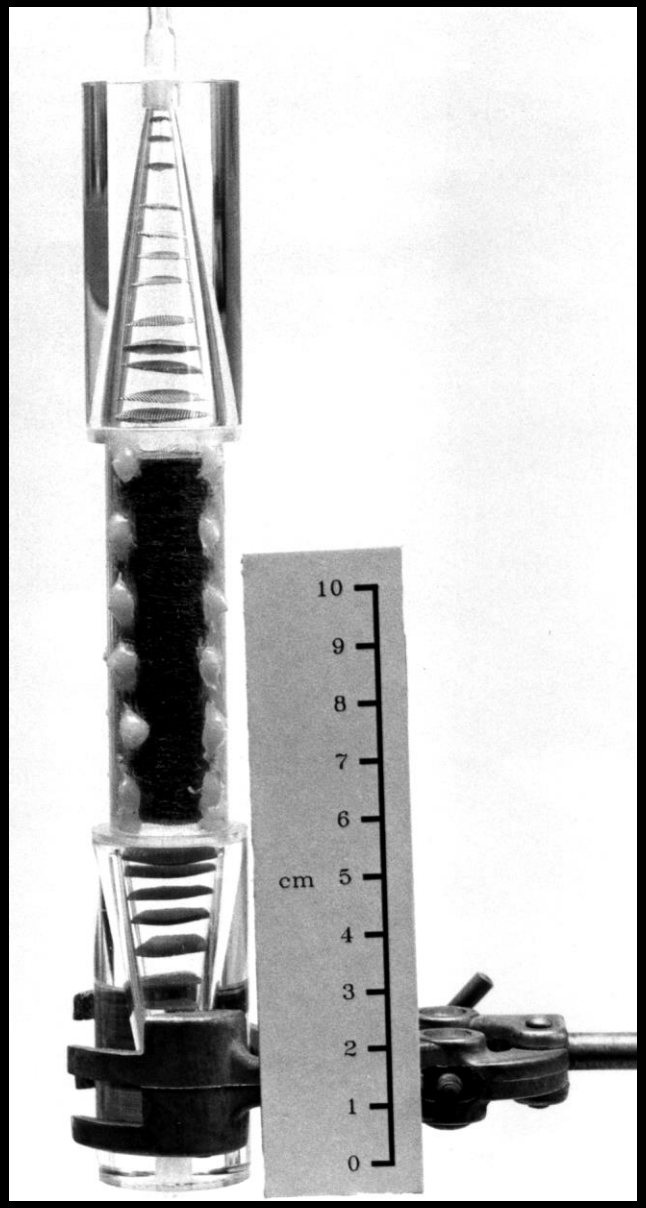

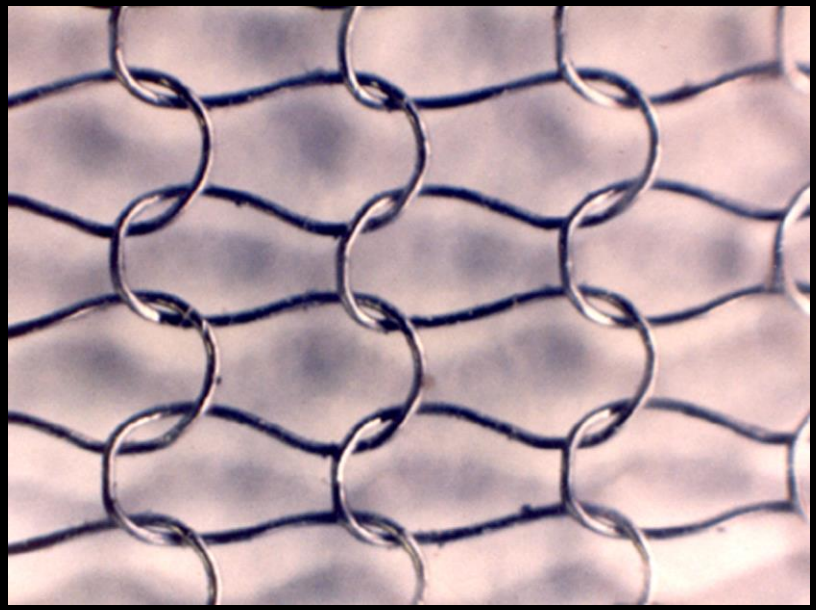

Matrix configurations - C was chosen as the best

Table 3.2 Wire Array Specifications.

Wire Array Construction.	Wire Diam. (μm)	Wire Type	F (%)	D_{mesh} or D_{random} (μm)	F_{Total} (%)	D_{2mesh} (μm)	Number of Layers
A 100 μm single strand wire arranged loosely as a woven mesh, spaced by 150 μm knitmesh.	100 150	SS430 SS430	3.0 3.4	715 1009	6.4	549	18
B 50 μm single strand wire arranged loosely as a woven mesh, spaced by 150 μm knitmesh.	50 150	SS430 SS430	3.1 6.7	349 670	9.8	289	36
C Layered 50 μm knitmesh.	50	SS430	3.1	352	---	---	120
D 50 μm knitmesh cut as a 13 mm wide strip and rolled into a solid cylinder.	50	SS430	3.0	358	---	---	Vertical Roll
E 22 μm single strand wire arranged loosely as a woven mesh, spaced by 150 μm knitmesh.	22 150	Fecralloy SS430	3.0 6.5	157 681	9.5	148	35
F 22 μm random array: 2-5 mm fibres loosely matted in three dimensions to form a very open fibre mat (Bekipor*), cut into circular sections and layered.	22	Fecralloy	2.7	210	---	---	Continuous
50 μm Layered 50 μm knitmesh.	50	SS430	1.8	477	---	---	73
100 μm 100 μm single strand wire arranged loosely as a woven mesh, spaced by 112 μm knitmesh.	100 112	SS430 SS304	3.9 2.7	616 844	5.8	471	25
150 μm Layered 150 μm knitmesh.	150	SS430	6.7	670	---	---	36

* Bekipor is supplied by N.V. Bekaert S.A., Zwevegem, Belgium.

Protocol

The separation system was slowly primed with 70% methanol since its low surface tension ensured that no air bubbles were trapped in the system. Distilled water then media were passed through. At the conclusion of the day's experiments the apparatus was flushed with Coulter Clenz followed by distilled water then 70% methanol. The apparatus was then dried by drawing air through it with a water jet vacuum pump. This cleaning ritual ensured that the separation system was in original condition every time it was used.

Evaluation

The performance of the separation was evaluated by considering the purity and the recovery (yield) of the positive (labelled) cells in the retained fraction. The depletion of the positive cells from the filtrate was also calculated as check on the recovery. The number and type of negative (unlabelled) cells retained by the filter was also determined. Cell balances were performed to ensure that all the cells could be accounted for.

Wire Array Comparison

Ficolled, cryopreserved cadaver bone marrow from one donor was labelled with tetrameric complexes consisting of 8G12 CD34 with DX1. The feed was 14% CD34 positive and 30% of the total cells were dead. Each filter was presented with 2×10^{7} cells in 5 ml at a bulk flow velocity of 2.4×10^{-5} m/s followed without stopping by 20 ml of media at 1.4×10^{-4} m/s (wash). The retained fraction was collected in 30 ml at 2.9×10^{-4} m/s.

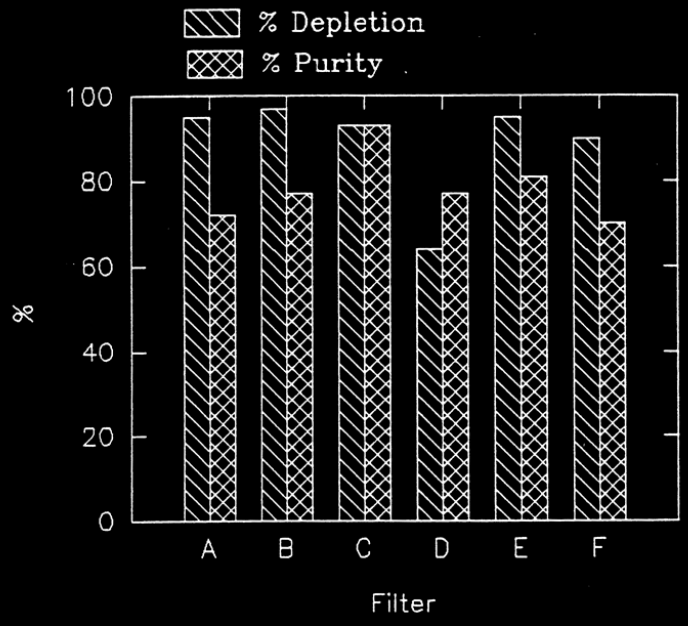

The %Depletion from the flow through fraction and the %Recovery to the retained fraction of the CD34 positive cells according to filter type.

Purity and Recovery

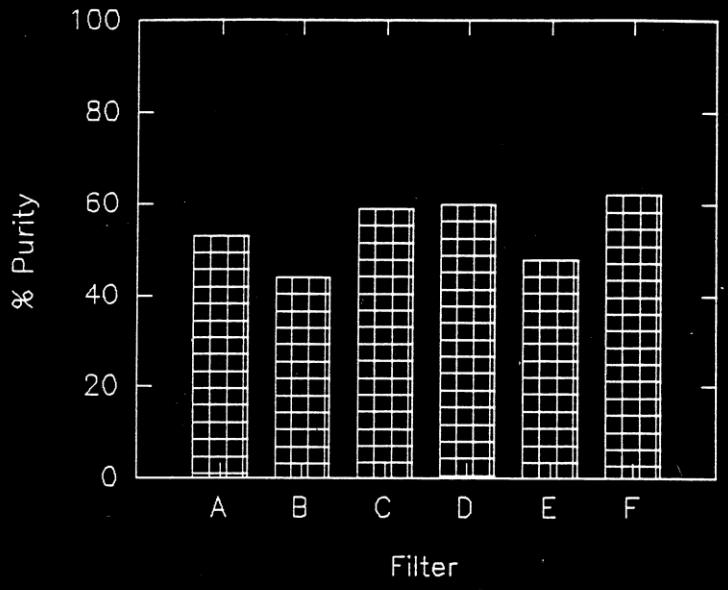

The %Purity of CD34 positive cells in the retained fraction with filter type.

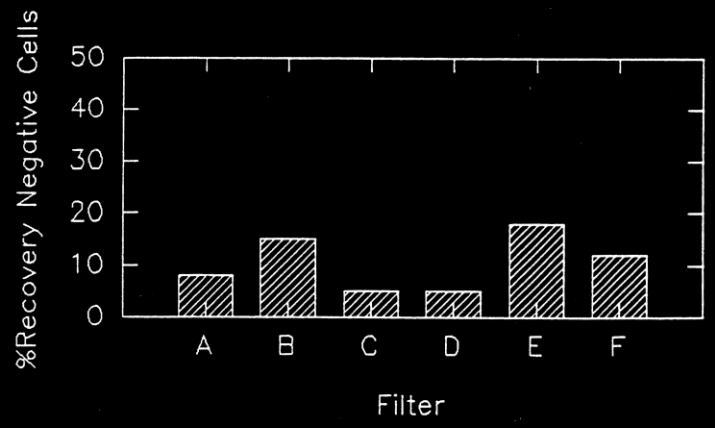

The %Recovery of negative cells to the retained fraction.

Brain repair

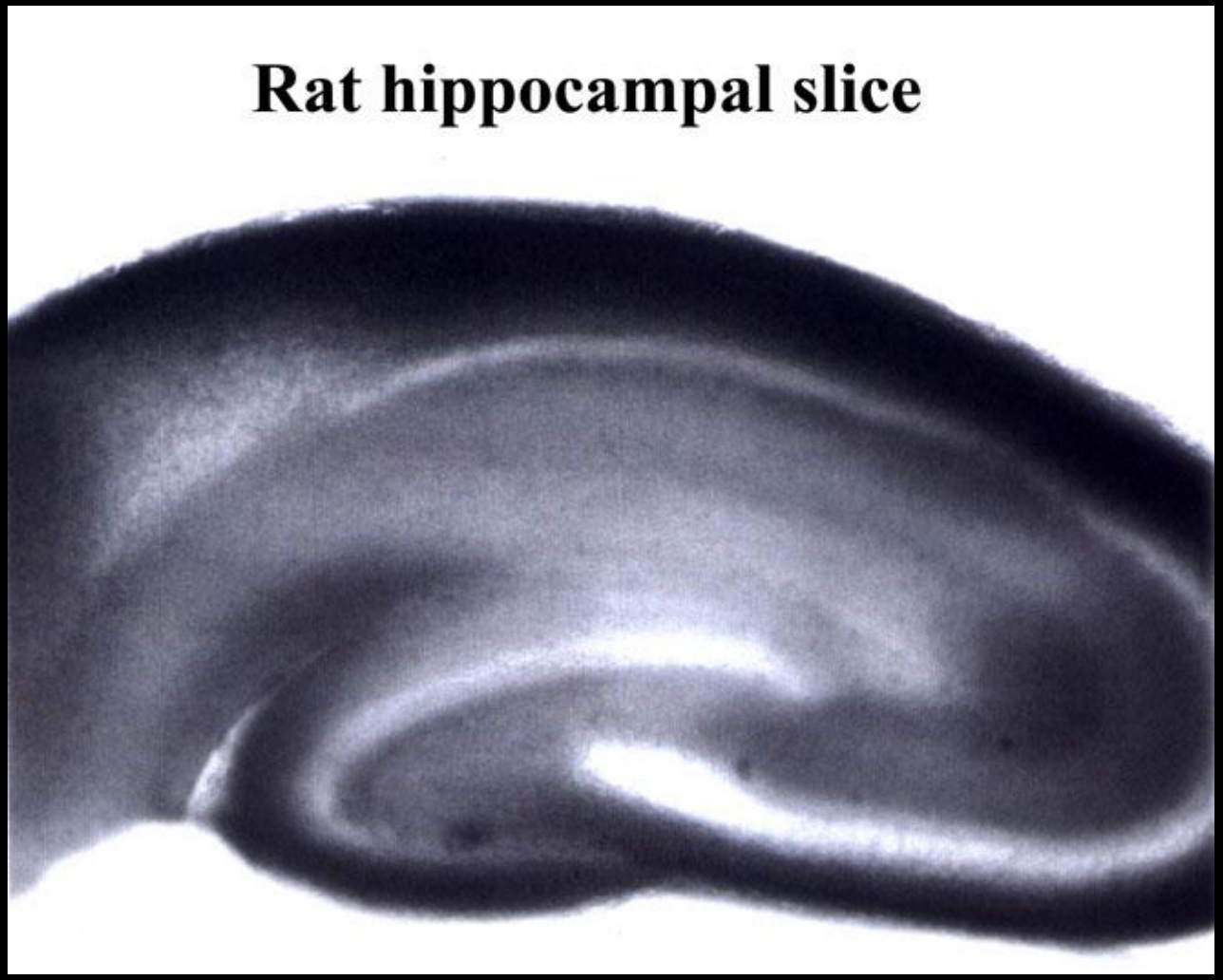

Structure of Hippocampus

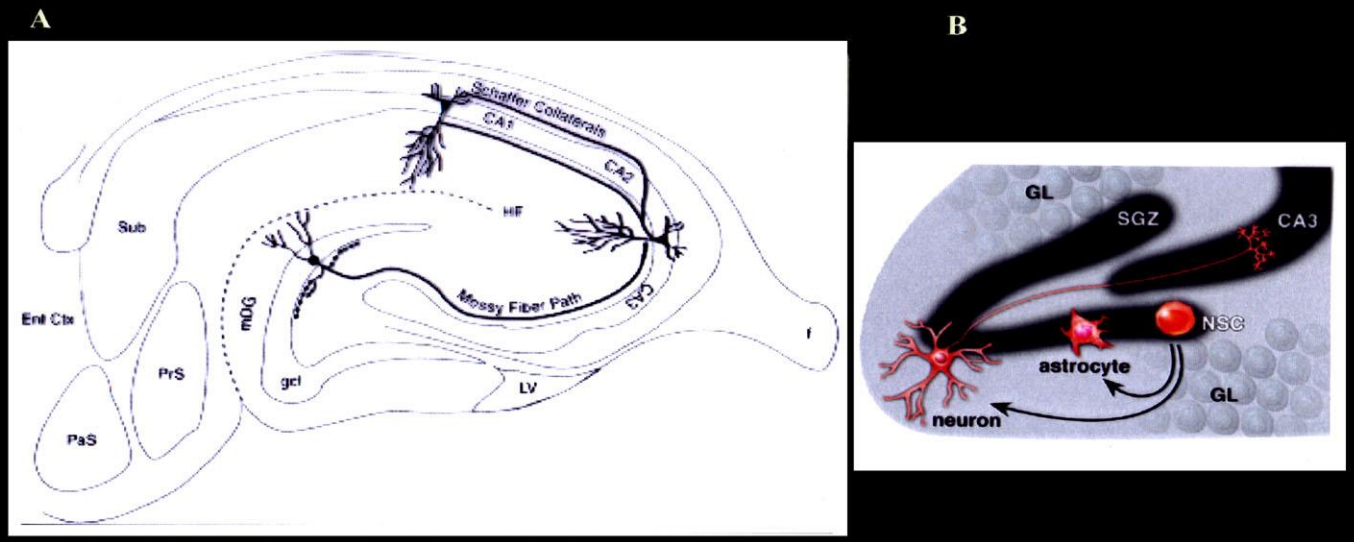

New neurons are continually added that contribute to the circuitry of the hippocampus. (A) Schematic representation of the circuitry of the hippocampal formation. The main information input to the hippocampus is via the perforant pathway from the entorhinal cortex (Ent Ctx) to granule cell dendrites of the dentate molecular layer (mDG), as well as pyramidal cells of CA3 and CA1. Granule cells (of the granule cell layer, gcl), in turn, project to area CA3 via the mossy fibers, whilst CA3 neurons project to area CA1. (B) The subgranular zone is a 2-3 cell layer lining the inner margin of the granule cell layer (GL), and contributes new neurons to the GL through the proliferation of neural stem cells (NSC), whose progeny can integrate into the existing circuitry (Hastings and Gould, 1999;Scharfman et al., 2000;van Praag et al., 2002) Abbreviations: f, fornix; HF, hippocampal fissure, LV, lateral ventricle; PaS, parasubiculum; PrS, presubiculum; Sub, subiculum proper. Images taken from (Hastings et al., 2001) & (Taupin and Gage, 2002).

Arrangement of magnets

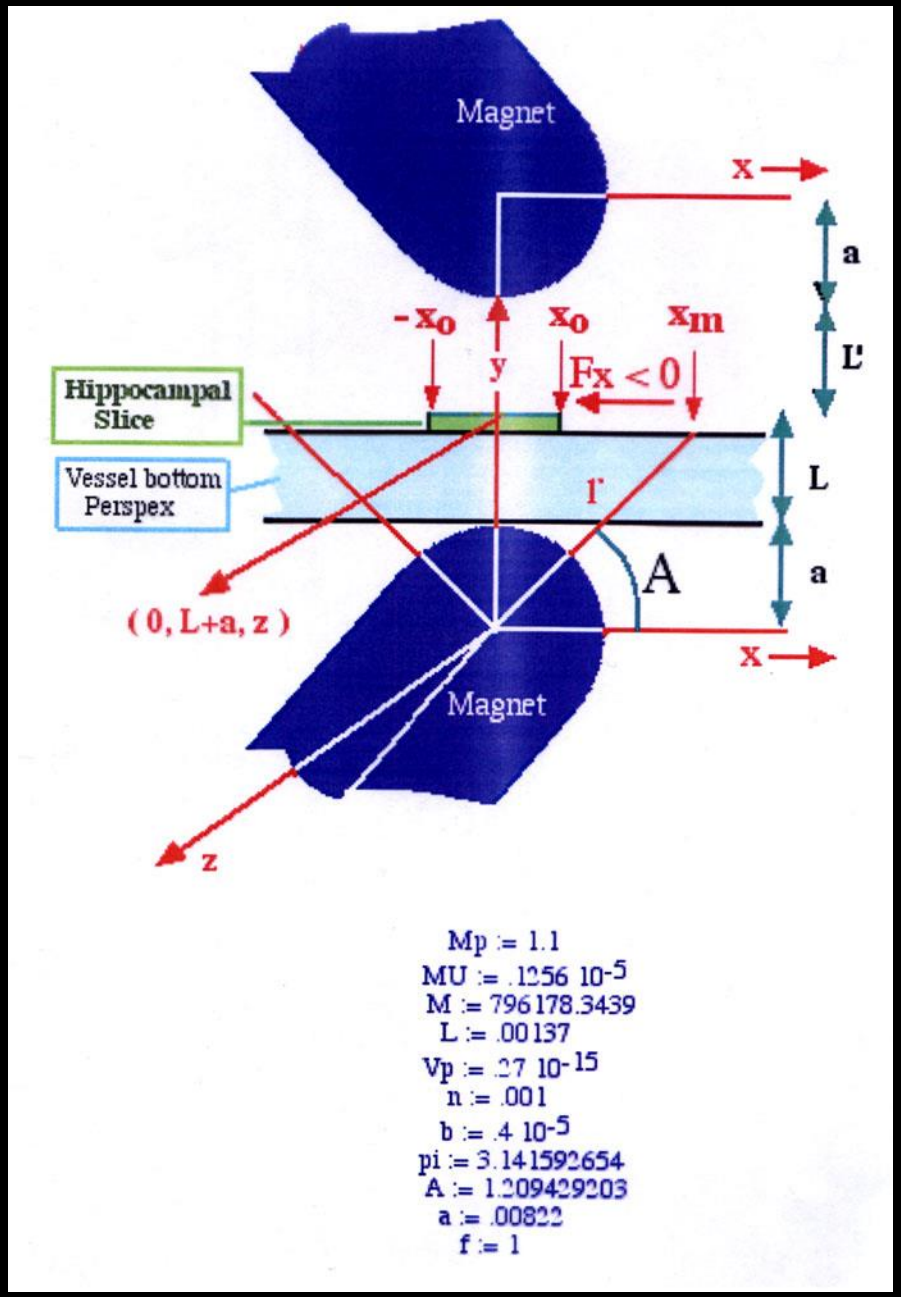

Magnetic Forces in x and z directions

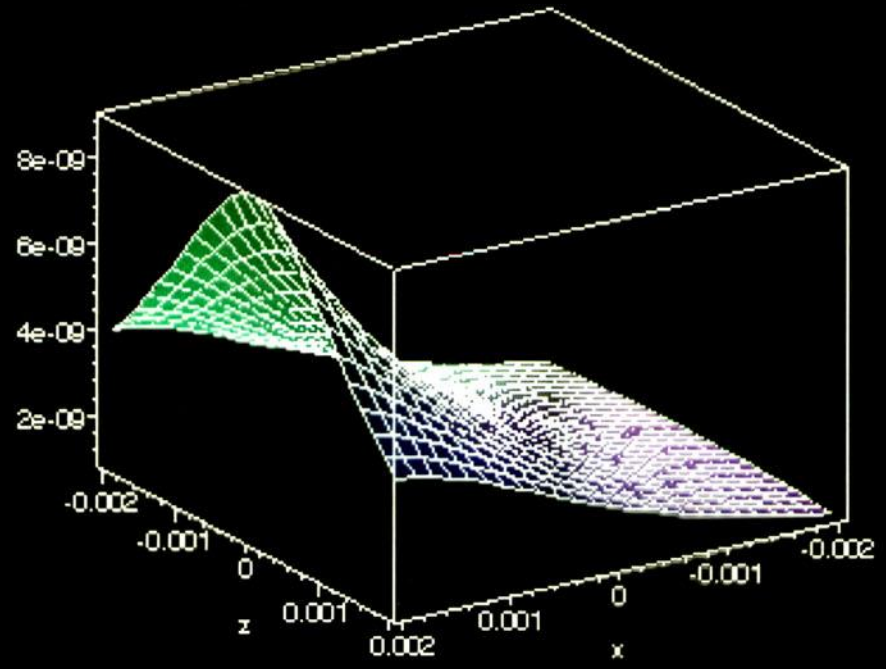

plot3d(-Fx,x=-0.002....0.002,z=-0.002....0.002);

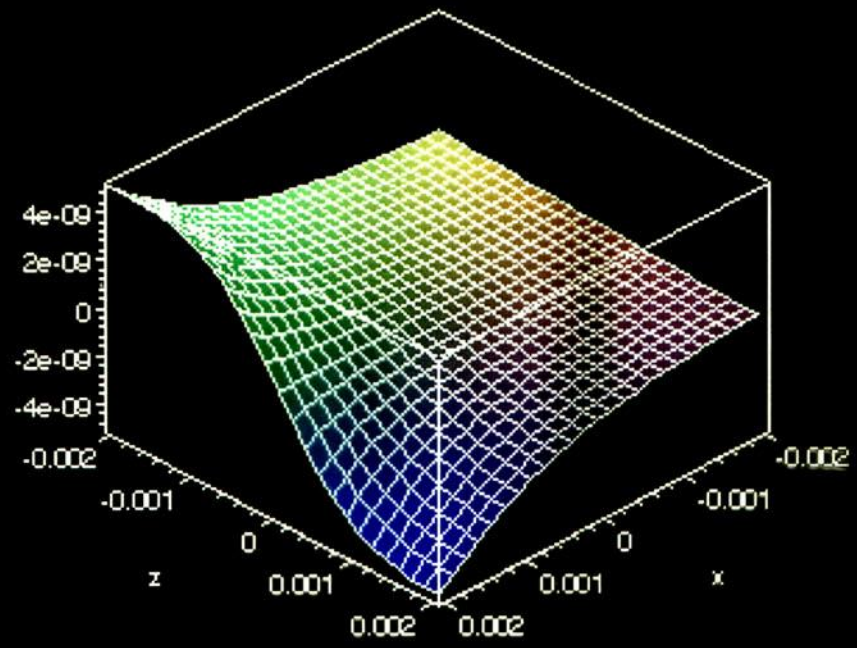

plot3d(Fz,x=-0.002....0.002,z=-0.002....0.002);